Chain Length Effects of Linear Alkanes in Zeolite Ferrierite. 1. Sorption and ^{13}C NMR Experiments[1]

Willy J. M. van Well,[†] Xavier Cottin,[†] Jan W. de Haan,[†] Berend Smit,[‡] Gautam Nivarthy,[§] Johannes A. Lercher,[§] Jan H. C. van Hooff,[†] and Rutger A. van Santen*,[†]

Schuit Institute of Catalysis, Laboratory for Inorganic Chemistry and Catalysis, Eindhoven University of Technology, P.O. Box 513, 5600 MB Eindhoven, The Netherlands; Department of Chemical Engineering, University of Amsterdam, Nieuwe Achtergracht 166, 1018 WV Amsterdam, The Netherlands; and Department of Chemical Technology, University of Twente, 7500 AE Enschede, The Netherlands

Received: December 3, 1997; In Final Form: March 5, 1998

Temperature-programmed desorption, heat of adsorption, adsorption isotherm, and ^{13}C NMR measurements are used to study the sorption properties of linear alkanes in ferrierite. Some remarkable chain length effects are found in these properties. While propane, *n*-butane, and *n*-pentane fill the ferrierite pore structure completely, *n*-hexane and *n*-heptane can only access a part of the pore structure. It is shown by ^{13}C NMR that *n*-hexane adsorbs only in the 10-ring channels of ferrierite and not in the ferrierite 8-ring cages. Adsorption of *n*-pentane in this cage is possible but only at relatively high pressures. At low pressures, only the 10-ring channels are filled by *n*-pentane. This remarkable sorption behavior is caused by the much lower heat of adsorption of *n*-pentane in the ferrierite 8-ring cage compared to the 10-ring channels and results in a two-stage desorption profile. In contrast to *n*-pentane, propane and *n*-butane adsorb easily into the complete pore structure, which is reflected in the normal single-stage desorption profile. The ^{13}C NMR measurements show furthermore that propane is preferentially adsorbed in the ferrierite 8-ring cage, while no clear preference is found for *n*-butane.

Introduction

The adsorption properties of reactants, intermediates, and products in zeolites are some of the parameters that greatly influence the performance of a zeolite catalyst. Many investigations have therefore been devoted to this subject. Especially the adsorption of hydrocarbons has attracted much attention since most of the applications of zeolite catalysts are in the petrochemical industry. The influence of the pore size and chemical composition of the zeolite on the heat of adsorption on one hand and the heat of adsorption as function of the chain length of the adsorbed molecule on the other hand has been widely studied.[2−6] Although the adsorption properties are in most cases simply proportional to the number of carbon atoms, the pore structure of the zeolite can cause important deviations from these linearities. Especially a pore structure of intersecting channels or cages can cause such deviations. The existence of these chain length effects has received relatively little attention in the literature.

In fact, the adsorption of *n*-alkanes in ZSM-5 is the only example where deviations from linearity in the adsorption properties have been studied in detail. In this system, *n*-hexane and *n*-heptane display a step in their adsorption isotherms and have a two-stage desorption profile. Longer and shorter *n*-alkanes have the normal type I isotherm and desorb in a single stage from ZSM-5.[6−8] Further, it was found that the pores of ZSM-5 are optimally filled by *n*-hexane and *n*-heptane.[7−9] All these phenomena can be related to the fit of the length of a segment of the zigzag channel of ZSM-5 with the length of the *n*-hexane and *n*-heptane molecules. This results at higher loadings in a so-called commensurate freezing of these molecules in the zigzag channels.[10]

Not only the adsorption properties but also the diffusion seem to be affected by the fit between the pore structure of the zeolite and the adsorbed molecules. It has for example been reported that an immobilization term has to be considered to obtain a correct description of the *n*-hexane diffusion in ZSM-5.[11,12]

In this work, we will study the adsorption of linear alkanes in ferrierite (FER), which has a pore structure consisting of intersecting channels and cages. We will focus on the possible existence of chain length effects in this system that will affect both the adsorption and diffusion properties. Ferrierite is an excellent catalyst for the isomerization of *n*-butene to isobutene, which is used for the production of methyl *tert*-butyl ether (MTBE).[13] Although the ferrierite-catalyzed isomerization of *n*-butene is widely studied, many aspects are still not fully understood. The pathway along which the isomerization proceeds and the role of coke formation are two important aspects that are still subject to debate.[14] A thorough knowledge of the adsorption properties of hydrocarbons in ferrierite is necessary to solve these questions and is, therefore, also of great importance from a catalytic point of view.

To study the (ad)sorption properties of linear alkanes, we will use temperature-programmed desorption (TPD) and adsorption experiments. The results of these experiments are compared to results from recently published adsorption isotherm measurements.[15] Moreover, ^{13}C NMR spectroscopy is used to study the location of the molecules in the pore structure of ferrierite. Results from molecular simulations are presented and compared to our experimental results in a subsequent publication.[16]

[†] Eindhoven University of Technology.
[‡] University of Amsterdam.
[§] University of Twente.

S1089-5647(98)00398-8 CCC: $15.00
Published on Web 04/23/1998

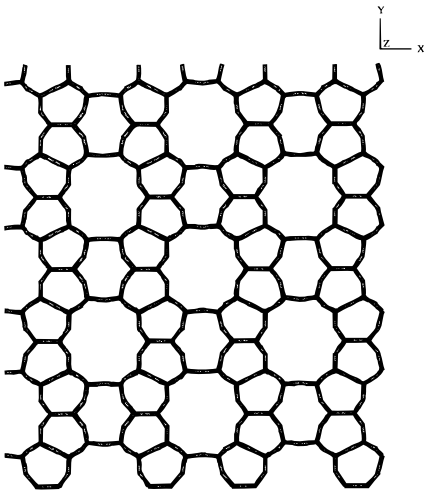

Figure 1. Two-dimensional pore structure of ferrierite viewed down [001] showing the 10-ring channels. In this figure, the ferrierite 8-ring cages interconnecting the 10-ring channels along [010] are viewed from above.

Experimental Section

Structure of Ferrierite. The zeolite ferrierite occurs in a natural form and can be made synthetically. The framework structure was first determined by Vaughan on a natural ferrierite with a Si/Al ratio of 5.5, containing sodium and magnesium as charge balancing cations.[17] The synthesis of the all-silica ferrierite has been reported by Kuperman recently.[18] The two-dimensional pore structure of ferrierite is displayed in Figure 1. It consists of straight 10-ring channels parallel to the *z*-axis which are interconnected by cages with 8-ring windows in the *y*-direction. The 10-ring channels have pore diameters of 5.4 × 4.2 Å. The diameter of the cages is about 7 Å, while the 8-ring windows of the cages have diameters of 4.8 × 3.5 Å.

Materials. Ferrierite (sample code CLA 27302) was provided by the Shell Research and Technology Center Amsterdam (The Netherlands). The sample has a Si/Al ratio of 9 and was obtained in the ammonium form. Ammonia was removed by calcination in a helium flow at 723 K. The NaZSM-22 sample (code JP 1505) was provided by Exxon Chemical Europe Inc. (Machelen, Belgium) and has a Si/Al ratio of 35. The sample was calcined in air for 48 h at a temperature of 773 K.

Propane 2.5 (purity 99.5%) and *n*-butane (purity 99.95%) were obtained from Hoek Loos (Schiedam, The Netherlands). The liquid *n*-alkanes (purity at least 99%) were obtained from Janssen Chimica (Geel, Belgium).

Temperature-Programmed Desorption. A Seteram TG-DSC 111 operated under a helium flow of about 3.0 L/h was used in these experiments. First, the sample was dehydrated by heating it to 723 K and holding it at that temperature for 10 min. Adsorption was performed at room temperature by adding a helium flow saturated with the sorbate or, in the case of propane and *n*-butane, a flow of pure sorbate to the pure helium flow of 3.0 L/h. Since the sorbate flow amounted to 0.8 L/h, adsorption was performed at a relative pressure of at most 0.2 (or in the case of propane and *n*-butane, a pressure of 20 kPa). After saturation was reached, the sorbate flow was switched off and the temperature program was started. A heating rate of 10 K/min was used up to a temperature of 723 K.

Adsorption Isotherm and Heat of Adsorption Measurement. A modified Seteram TG-DSC 111, which enables the measurement of adsorption isotherms, was used in these experiments. The sample was dehydrated by evacuation ($p < 10^{-7}$ kPa) at 673 K for 1 h. Pentane was discontinuously dosed to the system and equilibration was checked by observing the changes in both the heat flow and the weight. More details about the method and setup can be found elsewhere.[15] The isotherm of *n*-pentane in ferrierite was measured at 298 K at pressures from 10^{-4} to 1.3 kPa. The heat of adsorption was measured simultaneously with the adsorption isotherm up to a pressure of 1.3 kPa. Due to the limited range of pressure measurement, only the differential heat of adsorption was measured at higher pressures.

TABLE 1: Saturation Loadings and Occupied Pore Volumes of Linear Alkanes in H-FER at 293 K (Pressure of Propane and *n*-Butane, 20 kPa; Pressure of the Longer Alkanes, $p/p_0 = 0.2$)

	max. loading [g/g]	max. loading [mmol/g]	micropore volume [ml/g]
propane	0.072	1.6	0.15
n-butane	0.094	1.6	0.16
n-pentane	0.11	1.5	0.17
n-hexane	0.069	0.80	0.10
n-heptane	0.069	0.69	0.10

^{13}C CP MAS NMR Measurement. A vacuum system consisting of a calibrated volume connected to a Baratron pressure transducer and a turbo molecular pump was used for preparation of the samples for ^{13}C NMR measurements. A glass tube with a small capsule containing the sample (15−30 mg) was connected to the vacuum system. The sample was dehydrated by evacuation ($p < 10^{-4}$ kPa) and heating it to the required dehydration temperature (773 K for ferrierite, 723 K for NaZSM-22) and holding it at that temperature for at least 1 h. Next, a certain amount of sorbate was transferred into the calibrated volume and brought into contact with the dehydrated sample. After adsorption, the sample was cooled in liquid nitrogen and the capsule was melted off. The closed glass capsules with zeolite and adsorbed *n*-alkane were placed in a 7 mm MAS rotor and used in the NMR measurements.

The ^{13}C cross-polarized (CP) magic angle spinning (MAS) NMR measurements were performed on a Bruker MSL 400 at 9.4 T at room temperature. A MAS spinning rate of 2500 Hz was used. The contact time for cross polarization was 1 ms, while the repetition delay was 5 s. Different numbers of scans were accumulated depending on the amount of sample and on the loading of hydrocarbon on the sample. Adamantane was used as an external reference to transfer chemical shifts to the δ-scale. The free induction decays (FID) were weighted with a line broadening of 30 Hz prior to Fourier transformation; the resulting spectra were simulated using the WINFIT program of Bruker.

Results and Discussion

Temperature-Programmed Desorption. The loadings of the different *n*-alkanes at 293 K are displayed in Table 1. The occupied pore volume is given to enable a comparison between the different sorbates. The pore volume has been calculated by using the density of the liquid *n*-alkane at 293 K relative to water at 277 K. There is a large difference between the pore volumes occupied by the short *n*-alkanes and by *n*-hexane and *n*-heptane. Relatively low pore volumes occupied by longer *n*-alkanes (compared to the shorter *n*-alkanes) were also found in ZSM-5 and ascribed to a less efficient filling of the pores.[7,8] However, the differences found here are much larger and can therefore not be explained by differences in pore filling efficiencies. Such large differences suggest that less than the complete pore structure of ferrierite is available for long molecules such as *n*-hexane and *n*-heptane.

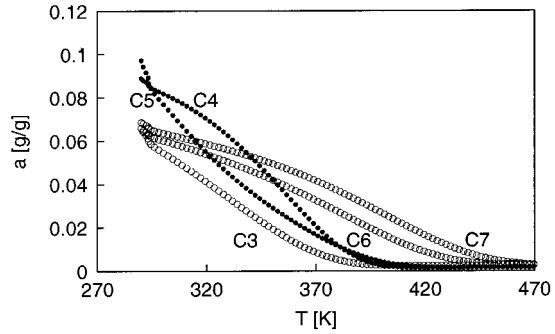

Figure 2. TPD curves of linear alkanes from H-FER.

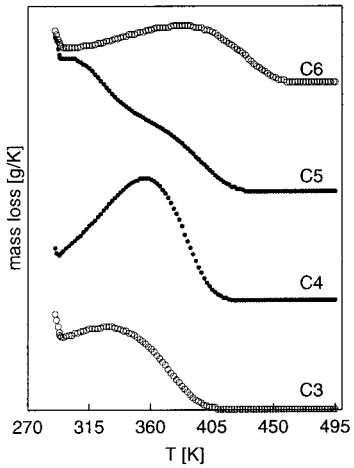

Figure 3. Differential mass loss (-d*m*/d*T*) of alkanes during TPD from H-FER.

Figure 2 shows the results of the TPD experiments as the residual amount of adsorbed *n*-alkane as a function of temperature. The two longest *n*-alkanes, *n*-hexane and *n*-heptane, show the usual desorption behavior: desorption in a single stage with the highest desorption temperature for the longest molecule. For both *n*-butane and *n*-pentane, the desorption starts at the higher loading. However, the desorption of *n*-pentane is much faster than the desorption of *n*-butane. The desorption profile of *n*-pentane is at high temperatures (low loadings) parallel to the desorption profiles of *n*-hexane and *n*-heptane, molecules that can only access a part of the ferrierite pore structure. This indicates that, at low loadings, also *n*-pentane adsorbs not in the complete pore structure. As a result of the fast initial desorption of *n*-pentane, the residual amount of adsorbed *n*-butane exceeds already at low temperatures the residual amount of adsorbed *n*-pentane. Only at very high temperatures does the *n*-butane loading fall again below the loading with *n*-pentane, which indicates that at low loadings *n*-butane is also adsorbed in all the ferrierite pores.

The differential mass loss (-d*m*/d*T*) curves derived from the desorption measurements of propane to *n*-hexane are given in Figure 3. The desorption curve of *n*-heptane (not displayed) is similar to the curve of *n*-hexane. The curves are separated from each other for the sake of clearness. The special desorption behavior of *n*-pentane becomes even clearer in this figure. While propane, *n*-butane, and *n*-hexane desorb in a single stage, *n*-pentane desorbs in two stages from the sample. The fast desorption of *n*-pentane results in a first desorption peak at a very low temperature, which occurs even before the desorption peak of propane. The temperatures at which the desorption of the different *n*-alkanes is maximal are shown in Table 2. The desorption peaks of *n*-butane and propane are at relatively high temperatures, the *n*-butane desorption peak is almost at the same temperature as the second desorption peak of *n*-pentane, and the difference in temperature between the propane desorption peak and the second *n*-pentane peak is about equal to the difference between this second *n*-pentane peak and the *n*-hexane desorption peak.

TABLE 2: Temperatures at the Differential Mass Loss Which Is Maximal

	T_1 [K]	T_2 [K]
propane		328
n-butane		356
n-pentane	302	357
n-hexane		382
n-heptane		401

TABLE 3: Loadings of Linear Alkanes at a Pressure of 1.3 kPa at 333 K and at 298 K As Reported by Eder et al.[15]

	$T = 333$ K	$T = 298$ K
propane	0.8	1.3
n-butane	1.1	1.5
n-pentane	0.6	1.1
n-hexane	0.6	0.7

Their relatively high desorption temperatures indicate that propane and *n*-butane are, in contrast to the longer molecules, at all loadings adsorbed in the entire ferrierite pore structure. The fast initial desorption of *n*-pentane shows that complete pore filling of ferrierite with *n*-pentane leads to highly constrained positions of the adsorbed *n*-pentane molecules. In contrast to *n*-pentane, propane and *n*-butane have easy access to the complete pore structure.

Comparison with Adsorption Isotherms at 333 K. Adsorption isotherms of *n*-alkanes ranging from propane to *n*-hexane were published recently by Eder et al.[15] The measurements were performed at 333 K, at pressures up to 1.3 kPa on an acidic ferrierite sample with a Si/Al ratio of 30. The loadings obtained at the maximum pressure of 1.3 kPa are displayed in Table 3. In this table, also the loadings reported at a temperature of 298 K and a pressure of 1.3 kPa are given.

The results in Table 3 show that the loadings obtained for *n*-hexane are distinctly lower than the loadings obtained for the shorter molecules. In contrast to propane and *n*-butane, the *n*-pentane loading is higher than the *n*-hexane loading only at 298 K and not at 333 K. The latter shows that *n*-pentane can fill the complete ferrierite pore structure only at relatively high pressures (or relatively low temperatures), while propane and *n*-butane fill the complete pore structure easily. Such a behavior is also shown in the isotherms measured by Eder et al. at 333 K[15] and is in full agreement with the TPD results. It is important to note that the *n*-butane isotherm measured crosses the *n*-pentane isotherm already at a low loading (about 0.2 mmol/g). This is in agreement with the result of the TPD measurements which indicate that the residual amount of adsorbed *n*-butane becomes lower than the amount of adsorbed *n*-pentane only at high temperatures.

Adsorption Isotherm and Heat of Adsorption of *n*-Pentane at 298 K. The *n*-pentane adsorption isotherm was measured at 298 K on the same ferrierite sample as used in the TPD experiments. It is displayed in Figure 4. The loading of about 1.1 mmol/g at a pressure of 1.3 kPa is in good agreement with the result reported by Eder et al. (see Table 3). Although *n*-pentane desorbs in two stages from this sample, no kinks or steps can be seen in the isotherm. On the basis of the TPD experiment we would expect such a step or kink at a loading of about 0.7 mmol/g, which is the loading between the two *n*-pentane desorption peaks. The adsorption isotherm is appar-

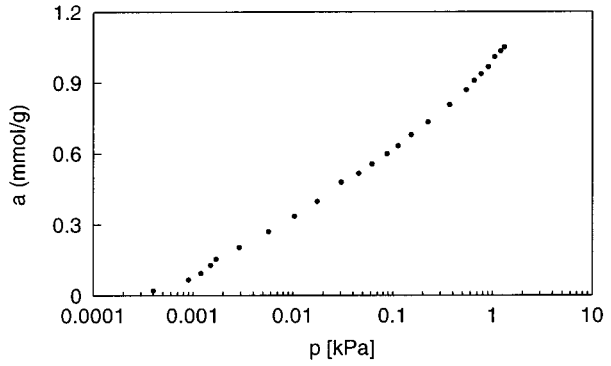

Figure 4. Adsorption isotherm of *n*-pentane in H-FER at 298 K.

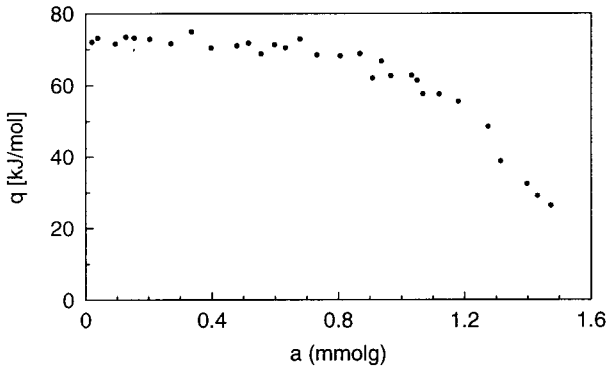

Figure 5. Isosteric heat of adsorption of *n*-pentane in H-FER at 298 K.

ently less sensitive to the microscopic adsorption behavior than TPD experiments are. This is comparable to the situation of *n*-hexane in ZSM-5, where the adsorption isotherm has only a small kink while there is a pronounced two-stage desorption profile.[7,8]

The corresponding isosteric heat of adsorption of *n*-pentane is displayed in Figure 5. It is clear that there is a large decrease of the heat of adsorption when loadings higher than 0.8 mmol/g are reached. This loading is in reasonable agreement with the loading of 0.7 mmol/g, where we expected a step or kink in the adsorption isotherm. The decrease in the heat of adsorption seems to be the cause of the two-stage desorption profile of *n*-pentane. The first desorption peak at high loading and low temperature is the result of the low heat of adsorption of *n*-pentane at high loadings. It should be noted that there is no such decrease in the heat of adsorption of *n*-butane for comparable loadings at 333 K, which agrees with the single-step desorption of *n*-butane.[15]

^{13}C CP MAS NMR Spectroscopy. For a full understanding of the results obtained from TPD and adsorption measurements, it is necessary to know the location of the alkane molecules in the ferrierite pores. A direct method to study the siting of hydrocarbons in zeolites is ^{13}C NMR because the carbon chemical shift is dependent on the medium or environment where the molecule is located. Boxhoorn et al. showed the influence of the zeolite environment by measuring the carbon chemical shift of the template tetrapropylammonium (TPA) occluded in ZSM-5.[19,20] They found a splitting of the methyl carbon atom signal and ascribed this to the difference between propyl groups pointing into the straight channels and propyl groups pointing into the zigzag channels. The effect of the medium on the chemical shift is dependent on the type of atom; it is generally stronger for methyl carbon atoms than for methylene carbon atoms.[21] Medium effects lead to higher chemical shift values (deshielding) as the medium or environment has a larger dielectric constant.[21,22] For molecules located in zeolites the chemical shift value increases when the molecules are located in smaller cavities or narrower channels. This was demonstrated by Hayashi and co-workers, who showed that the carbon chemical shift of tetramethylammonium (TMA) adsorbed or occluded in different zeolite cages decreases when the size of the cage increases.[23] The results of Hayashi et al. are in perfect agreement with earlier work of Jarman and co-workers, who were able to make a distinction in zeolite ZK-4 between TMA occluded in the sodalite cage and TMA in the α-cage by means of ^{13}C NMR.[24] It was shown in all three examples that the chemical composition of the zeolite has only a negligible influence on the carbon chemical shift.

TABLE 4: ^{13}C NMR Chemical Shifts of *n*-Hexane in H-FER and NaZSM-22 at Different Loadings

zeolite	loading [mmol/g]	$\delta(CH_3)$	$\delta(CH_2)$	$\delta(CH_2)$
H-FER	0.8	14.0	23.9	33.3
H-FER	0.3	13.4	24.3	33.7
NaZSM-22	0.7	13.7	23.5	32.7
NaZSM-22	0.4	13.3	23.8	33.3

Apart from medium effects, ^{13}C NMR chemical shifts of *n*-alkanes adsorbed in zeolites are also influenced by the conformational equilibrium of the *n*-alkane. Increasing contributions of gauche conformers lead to lower chemical shift values (shielding) in analogy with the situation in, for example, polymers.[25] The difference in chemical shift between a trans and a gauche bond is at most 5 ppm and depends on the position of the carbon atom in the chain.[21] As a consequence, in our study propane is the only molecule where only the environment of the adsorbed molecule influences the chemical shift.

We have used NaZSM-22 as a "reference" zeolite to enable a distinction between molecules adsorbed in the 10-ring channels from molecules adsorbed in the ferrierite cages. The pore structure of NaZSM-22 (structural code TON) consists only of 10-ring channels with a diameter of 4.4 × 5.5 Å. Since the 10-ring channels of ZSM-22 and ferrierite possess similar dimensions, it is to be expected that the influence of the adsorption environment on the chemical shift of the *n*-alkanes adsorbed in the 10-ring channel is similar for these two zeolites. Configurational-bias Monte Carlo (CB-MC) simulations have predicted that the conformations of *n*-alkanes adsorbed in zeolites are determined by the size of the cage or the diameter of the channel where the molecule is located.[26] The conformations of molecules adsorbed in the two different, but similar, 10-ring channels are thus assumed to be comparable. Therefore, we expect the chemical shifts of the molecules adsorbed in the 10-ring channel of NaZSM-22 or in the 10-ring channel of H-FER to be about equal. Our choice of ZSM-22 as a reference for the 10-ring channels of ferrierite is supported by results of Forbes and Rees on diethanolamine (DEA) as template in the synthesis of ZSM-22, ferrierite, and ZSM-5.[27] They found that the ^{13}C NMR chemical shifts of the protonated DEA in as-synthesized samples of ZSM-22 and FER are about equal, which supported their assumption that DEA is located only in the 10-ring channel of ferrierite.

Samples with different loadings of *n*-alkanes were measured to study the siting as a function of loading. Figures 6−9 display the ^{13}C NMR spectra of *n*-hexane, *n*-pentane, *n*-butane, and propane adsorbed in NaZSM-22 and in H-FER. The corresponding chemical shift values are given in Tables 4−7.

Three signals corresponding to the three different carbon atoms are found in the spectra of *n*-hexane adsorbed in H-FER as displayed in Figure 6. All three signals correspond well with the signals measured for *n*-hexane in NaZSM-22. This resem-

TABLE 5: ^{13}C NMR Chemical Shifts of *n*-Pentane in H-FER and NaZSM-22 at Different Loadings. The Results for H-FER Are Differentiated to *n*-Pentane Adsorbed in the 10-Ring Channel and in the 8-Ring Cage

zeolite	loading [mmol/g]	$\delta(CH_3)$ channel	$\delta(CH_3)$ cage	$\delta(CH_2)$ channel	$\delta(CH_2)$ cage	$\delta(CH_2)$ channel	$\delta(CH_2)$ cage
H-FER	1.5	14.2	15.9	23.9	22.2	34.4	32.1
H-FER	1.2	14.0	15.8	23.7	22.0	34.6	32.6
H-FER	0.8	13.8	15.8	23.8	21.9	34.8	32.1
H-FER	0.4	13.7		23.8		34.8	
NaZSM-22	0.3	13.6		24.2		35.6	
NaZSM-22	0.2	13.5		23.8		35.5	

TABLE 6: ^{13}C NMR Chemical Shifts of *n*-Butane in H-FER and NaZSM-22 at Different Loadings. The Results for H-FER Are Differentiated to *n*-Butane Adsorbed in the 10-Ring Channel and in the 8-Ring Cage

zeolite	loading [mmol/g]	$\delta(CH_3)$	$\delta(CH_2)$ channel cage	
H-FER	1.6	13.9	25.8	24.5
H-FER	1.1	13.8	25.9	24.6
H-FER	0.5	13.5	25.9	24.4
H-FER	0.2	13.5	25.9	24.3
NaZSM-22	0.8	14.1	25.5	
NaZSM-22	0.5	13.9	25.7	

TABLE 7: ^{13}C NMR Chemical Shifts of Propane in H-FER and NaZSM-22 at Different Loadings. The Results for H-FER Are Differentiated to Propane Adsorbed in the 10-Ring Channel and in the 8-Ring Cage

zeolite	loading [mmol/g]	$\delta(CH_3) + \delta(CH_2)$ channel	$\delta(CH_3) + \delta(CH_2)$ cage
H-FER	1.8	16.1	17.0
H-FER	1.1	15.8	17.0
H-FER	0.6	15.8	17.0
H-FER	0.3	15.9	17.1

zeolite	loading [mmol/g]	$\delta(CH_3)$ channel	$\delta(CH_2)$ cage
NaZSM-22	0.5	15.2	16.2
NaZSM-22	0.2	15.2	16.3

blance indicates clearly that *n*-hexane adsorbs only in the 10-ring channels of ferrierite. This is also reasonable in view of the limited volume of the ferrierite cage. The volume of this cage is limited because its largest window consists of a narrow ring of eight oxygen atoms with a diameter comparable to the kinetic diameter of an *n*-alkane molecule. Longer molecules, with a larger molecular volume, like *n*-hexane, can therefore not adsorb in these cages. It agrees also with the finding that the loading of *n*-hexane in ZSM-22 is not lower than the loading of shorter alkane molecules.[15] The good agreement between the signals found for H-FER and NaZSM-22 shows furthermore that our assumption that NaZSM-22 can be used as a reference zeolite is correct.

Figure 7 displays the spectra of *n*-pentane adsorbed in H-FER and in NaZSM-22. Three signals, which agree well with the signals found for *n*-pentane in NaZSM-22, are found in the spectrum of 0.4 mmol/g of *n*-pentane in H-FER, showing that adsorption of *n*-pentane is initially limited to the 10-ring channels of H-FER. An additional set of three signals appears at higher loadings. These additional signals increase with increasing loading of *n*-pentane and differ by at least 2 ppm from the signals found for *n*-pentane adsorbed in NaZSM-22. Obviously, adsorption of *n*-pentane in the 8-ring cages of H-FER takes place only at higher loadings.

While the methyl signal of *n*-pentane located in the 8-ring cage is deshielded from the methyl signal of *n*-pentane in the

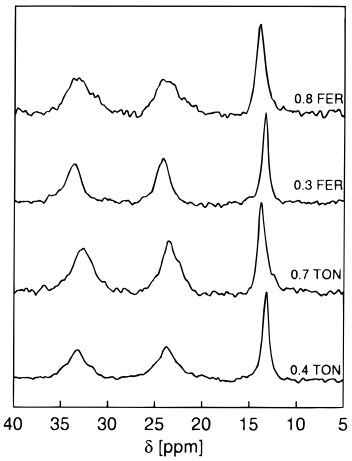

Figure 6. ^{13}C NMR spectra of *n*-hexane in H-FER and NaZSM-22 (TON) at different loadings, indicated in units of mmol/g in the spectra.

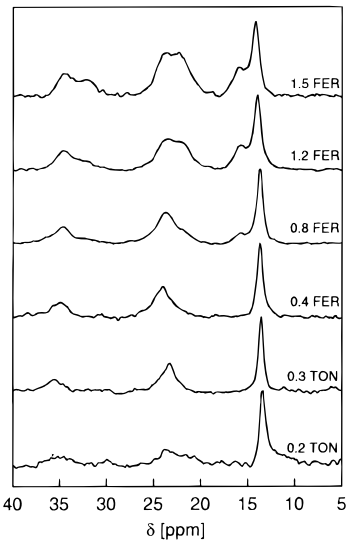

Figure 7. ^{13}C NMR spectra of *n*-pentane in H-FER and NaZSM-22 (TON) at different loadings, indicated in units of mmol/g in the spectra.

10-ring channels, the methylene signals corresponding to the 8-ring cage are shielded. This opposite order shows that there are two opposing effects on the carbon chemical shift when we compare *n*-pentane in the ferrierite 8-ring cage with *n*-pentane in the 10-ring channels. These two effects are the adsorption environment and the conformation of the *n*-alkane molecule. Computer simulations predicted that *n*-alkanes adsorbed in the ferrierite 8-ring cage are highly coiled (many gauche conformations), while they are highly stretched in the 10-ring channels (many trans conformations).[26] Coiling of *n*-pentane will lead to shielding of all three ^{13}C NMR signals of *n*-pentane.[21,25] An increase of the medium effect will, however, cause deshielding, particularly for the methyl signals.[21,22] We interpret our ^{13}C NMR results as follows: the *n*-pentane molecules are significantly more coiled in the 8-ring cages than in the 10-ring channels, as evidenced by the shielding of both methylene signals. For the methyl groups, this effect is more than compensated for by the strongly increased medium effects, leading to a net deshielding (in the cages with respect to the channels). This means that *n*-pentane molecules adsorbed in the 8-ring cages are in a tighter environment than *n*-pentane molecules adsorbed in the 10-ring channel.

Adsorption of *n*-butane in H-FER leads at all the loadings measured here to three signals in the NMR spectrum: one signal

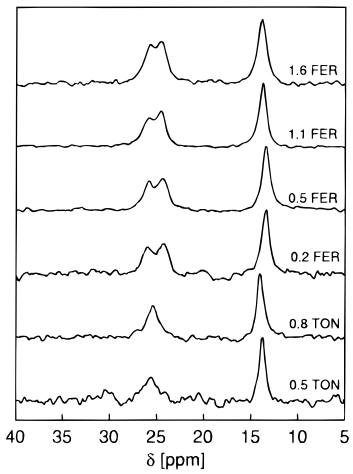

Figure 8. ^{13}C NMR spectra of *n*-butane in H-FER and NaZSM-22 (TON) at different loadings, indicated in units of mmol/g in the spectra.

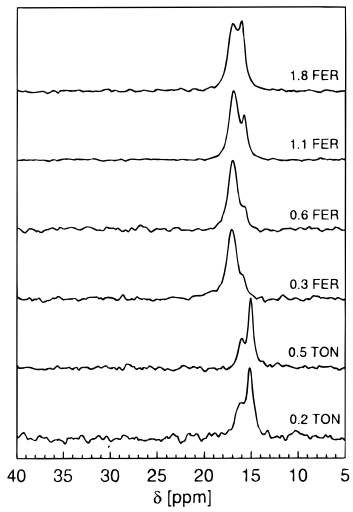

Figure 9. ^{13}C NMR spectra of propane in H-FER and NaZSM-22 (TON) at different loadings, indicated in units of mmol/g in the spectra.

for the methyl group and two signals for the methylene group (see Figure 8). The methylene signal that occurs at the highest chemical shift value and the methyl signal agree very well with the signals found for *n*-butane in NaZSM-22. The two signals for the methylene group show that there is a distribution of *n*-butane over the 10-ring channels and 8-ring cages at all loadings. Since we are dealing with two opposing effects on the carbon chemical shift (see above), it is very well possible that the methyl signal, where the medium effect is largest, in fact consists of two overlapping signals. This would mean that the deshielding (medium effect) upon comparing 8-ring cages with 10-ring channels is smaller for the methyl groups of *n*-butane than for the methyl groups of *n*-pentane. This is logical since the shorter *n*-butane molecules will have more free space left and are, thus, in a less tight environment than the *n*-pentane molecules in the ferrierite 8-ring cage.

Figure 9 shows the spectra of propane in H-FER and in NaZSM-22. The two signals found in the latter zeolite in a ratio of about 1:2 (at all loadings) are assigned to the methylene and methyl carbon atoms, respectively, in analogy with the gas phase.[28] All spectra of propane adsorbed in H-FER show two signals; the contribution of the signal at the lowest chemical shift increases clearly with increasing loading. While this signal appears only as a small shoulder at the lowest loading, it is about equal to the other signal when the pores of H-FER are filled completely. Because of this pronounced variation with loading, we do not ascribe the two signals to the two different carbon atoms but to the two different adsorption sites. Figure 9 shows therefore that propane is at all loadings distributed over two different adsorption sites, but also that propane has a strong preference for one of these two sites. The propane signal in H-FER with the lowest chemical shift falls between the two (methyl and methylene) signals of propane in NaZSM-22 and is thus ascribed to propane in the 10-ring channel of H-FER. The signal occurring at the highest chemical shift value is consequently assigned to propane located in the 8-ring cage. Its position is indeed very different (by respectively 1.8 and 0.8 ppm) from the positions of the methyl and methylene signals of propane in NaZSM-22. This interpretation implies that propane has a strong preference for adsorption in the 8-ring cage. The deshielding of the signals of propane adsorbed in the 8-ring cages agrees with our earlier conclusion that the molecules are in a tighter environment in the 8-ring cages than in the 10-ring channels. It should finally be noted that the occurrence of two different sets of NMR signals indicates that the exchange of molecules between the 10-ring channels and the 8-ring cages is very slow. This confirms the existence of a large barrier (about 100 kJ/mol) for diffusion of linear butene molecules through the 8-ring window as calculated by Jousse and co-workers.[29]

Conclusions

The results obtained from temperature-programmed desorption, adsorption isotherms, and heat of adsorption measurements are in good agreement with each other and with the earlier published adsorption isotherms. It is shown by ^{13}C CP MAS NMR that only short alkanes up to *n*-pentane can access the full two-dimensional pore structure of ferrierite. Longer alkanes adsorb only in the 10-ring channels and can therefore only access a one-dimensional pore structure. This difference in accessibility of the pore structure will most probably have a large effect on the diffusion of molecules with different chain lengths in ferrierite. In this context, it is interesting to note that the formation of coke in the ferrierite pores is necessary to suppress the production of long chain molecules in the ferrierite-catalyzed *n*-butene isomerization process.[13] The results presented here imply that the diffusion of long chain molecules out of the ferrierite pores will be much more hindered by the formation of coke than the diffusion of the short chain molecules since these longer molecules can exploit only a one-dimensional pore structure.

Temperature-programmed desorption measurements have shown that propane and *n*-butane have easy access to the complete pore structure, while the *n*-pentane molecules are highly constrained at complete pore filling. This constrained position results in a two-stage desorption, with the first *n*-pentane desorption peak occurring at a very low temperature. The desorption at low temperature is the result of a low heat of adsorption at higher *n*-pentane loadings. This stands in contrast to the two-stage desorption of *n*-hexane and *n*-heptane from ZSM-5, which is caused by a difference in adsorption entropies.[7,9,30]

It is concluded for ^{13}C NMR that long alkanes such as *n*-hexane adsorb only in the 10-ring channels of ferrierite. They are excluded from the ferrierite 8-ring cage due the limited volume of the cage. The adsorption of *n*-pentane initially takes place only in the 10-ring channel; adsorption into the ferrierite

8-ring cage occurs only at higher loadings. This result, combined with the decrease of the heat of adsorption at higher loadings, means that the heat of adsorption of *n*-pentane in the ferrierite 8-ring cage is distinctly lower than in the 10-ring channels.

The two shortest alkanes measured, propane and *n*-butane, are at all loadings distributed over the channels and 8-ring cages. While propane adsorbs preferentially in the ferrierite 8-ring cage, no clear preference is found for *n*-butane. It can be concluded from the NMR measurements that the molecules adsorbed in the ferrierite 8-ring cage are in a tighter environment than the molecules adsorbed in the 10-ring channel of ferrierite.

In part 2, we will show that there is good agreement between the experimental results presented here and the results of molecular simulations of the adsorption of linear alkanes in ferrierite.[16] Moreover, we will use the experimental results to set the limits to the parameters used in the simulations that describe the interaction between the *n*-alkane molecules and the zeolite framework.

Acknowledgment. W.J.M.v.W. is indebted to the Stichting Scheikundig Onderzoek in Nederland (SON). Netherlands Institute for Research in Catalysis (NIOK) publication #TUE 98-5-03.

References and Notes

(1) Part of this work was communicated previously: van Well, W. J. M.; Cottin, X.; de Haan, J. W.; van Santen, R. A.; Smit, B. *Angew. Chem., Int. Ed. Engl.* **1998**, *37*, 1081.

(2) Stach, H.; Lohse, U.; Thamm, H.; Schirmer, W. *Zeolites* **1986**, *6*, 74.

(3) Stach, H.; Fiedler, K.; Jänchen, J. *Pure Appl. Chem.* **1993**, *65*, 2193.

(4) Smit, B.; Siepmann, J. I. *Science* **1994**, *264*, 1118.

(5) Bates, S. P.; van Well, W. J. M.; van Santen, R. A.; Smit, B. *J. Am. Chem. Soc.* **1996**, *118*, 6753.

(6) Eder, F.; Lercher, J. A. *Zeolites* **1997**, *18*, 75.

(7) van Well, W. J. M.; Wolthuizen, J. P.; Smit, B.; van Hooff, J. H. C.; van Santen, R. A. *Angew. Chem., Int. Ed. Engl.* **1995**, *34*, 2543.

(8) van Well, W. J. M.; Wolthuizen, J. P.; Smit, B.; van Hooff, J. H. C.; van Santen, R. A. *Stud. Surf. Sci. Catal.* **1997**, *105*, 2347.

(9) Sun, M. S.: Talu, O.; Shan, D. B. *J. Phys. Chem.* **1996**, *100*, 17276.

(10) Smit, B.; Maesen, T. L. M. *Nature* **1995**, *374*, 42.

(11) Micke, A.; Bülow, M.; Kocirík, M.; Struve, P. *J. Phys. Chem.* **1994**, *98*, 12337.

(12) Song, L.; Rees, L. V. C. *J. Chem. Soc., Faraday Trans.* **1997**, *93*, 649.

(13) Mooiweer, H. H.; de Jong, K. P.; Kraushaar-Czarnetzki, B.; Stork, W. H. J.; Krutzen, B. C. H. *Stud. Surf. Sci. Catal.* **1994**, *84*, 2327.

(14) Mériaudeau, P.; Tuan, V. A., Le, N. H.; Szabo, G. *J. Catal.* **1997**, *169*, 397.

(15) Eder, F.; Lercher, J. A. *J. Phys. Chem. B* **1997**, *101*, 1273.

(16) van Well, W. J. M.; Cottin, X.; van Hooff, J. H. C.; van Santen, R. A.; Smit, B. *J. Phys. Chem. B* **1998**, *102*, 3952.

(17) Vaughan, P. A. *Acta Crystallogr.* **1966**, *21*, 983.

(18) Kuperman, A.; Nadimi, S.; Oliver, S.; Ozin, G. A.; Garcés, J. M.; Olken, M. M. *Nature* **1993**, *365*, 239.

(19) Boxhoorn, G.; van Santen, R. A.; van Erp, W. A.; Hays, G. R.; Huis, R.; Clague, D. *J. Chem. Soc., Chem. Commun.* **1982**, 264.

(20) Boxhoorn, G.; van Santen, R. A.; van Erp, W. A.; Hays, G. R.; Alma, N. C. M.; Huis, R.; Clague, A. D. H. *Proceedings of the 6th International Zeolite Conference*; 1984, p 694.

(21) van de Ven, L. J. M.; de Haan, J. W.; Bucinská, A. *J. Phys. Chem.* **1982**, *86*, 2516.

(22) Rummens, F. H. A. In *NMR Basic Principles and Progress, Vol. 10: van der Waals Forces and Intermolecular Shielding Effects*; Diehl, P., Fluck, E., Kosfeld, R., Eds.; Springer-Verlag: Berlin, 1975.

(23) Hayashi, S.; Suzuki, K.; Shin, S.; Hayamizu, K.; Yamamoto, O. *Chem. Phys. Lett.* **1985**, *113*, 368.

(24) Jarman, R. H.; Melchior, M. T. *J. Chem. Soc., Chem. Commun.* **1984**, 414.

(25) Tonelli, A. E. *NMR Spectroscopy and Polymer Microstructure: The Conformational Connection*; VCH Publishers: Cambridge, 1989.

(26) Bates, S. P.; van Well, W. J. M.; van Santen, R. A.; Smit, B. *J. Phys. Chem.* **1996**, *100*, 17573.

(27) Forbes, R. N.; Rees, L. V. C. *Zeolites* **1995**, *15*, 444.

(28) van de Ven, L. J. M.; de Haan, J. W. *Chem. Commun.* **1978**, 94.

(29) Jousse, F.; Leherte, L.; Vercauteren, D. P. *Mol. Simul.* **1996**, *17*, 175.

(30) Olson, D. H.; Reischman, P. T. *Zeolites* **1996**, *17*, 434.